EurJIC
European Journal of Inorganic Chemistry

Research Article
doi.org/10.1002/ejic.202200161

Chemistry Europe
European Chemical Societies Publishing

www.eurjic.org

Synthesis, Structure and Thermal Properties of Volatile Indium and Gallium Triazenides**

Rouzbeh Samii,[a] Sydney C. Buttera,[b] Vadim Kessler,[c] and Nathan J. O'Brien*[a]

Indium and gallium nitride are important semi-conductor materials with desirable properties for high-frequency and power electronics. We have previously demonstrated high-quality ALD grown InN and GaN using the hexacoordinated 1,3-diisopropyltriazenide In(III) and Ga(III) precursors. Herein we report the structural and thermal properties their analogues employing combinations of isopropyl, *sec*-butyl and *tert*-butyl-triazenide alkyl groups on the exocyclic nitrogen of the triazenide ligand. The new triazenide compounds were all found to be volatile (80-120 °C, 0.5 mbar) and showed very good thermal stability (200 and 300 °C). These new triazenide analogues provide a set of precursors whose thermal properties are determined and can be accordingly tailored by strategic choice of exocyclic nitrogen alkyl substituents.

Introduction

The electron mobility of indium nitride (InN) makes it highly suitable as the conduction channel in gallium nitride (GaN) based high electron mobility transistors.[1,2] Implementation of these materials into future microelectronic devices requires high-quality thin films with low impurity levels. Electronic grade GaN is routinely deposited by chemical vapour deposition (CVD) at 800–1000 °C using trimethylgallium and NH_3.[3] This process is not transferrable to InN as it decomposes into metallic In and N_2 gas above 500 °C.[4] Atomic layer deposition (ALD) is a low temperature variant of CVD that relies solely on self-limiting surface chemical reactions in order to obtain higher control, both in film thickness and composition, for material deposition.[5] To obtain high-quality ALD films, the metal precursor must have desirable physical and chemical properties. The precursor must be sufficiently volatile under deposition conditions to ensure enough of it reaches the growth region. It must also be thermally stable to prevent gas-phase decomposition reactions that result in continuous film growth or contamination at the growing film surface. The precursor should react reliably and predictably with the surface species during film growth to form a stable monolayer. To avoid incorporating impurities into the growing film, the ligand fragments of the chemisorbed precursor should be non-reactive and volatile enough to be removed by an intermittent purge pulse.

Trimethylindium and trimethylgallium are commonly used for ALD of InN[6–9] and GaN,[10–15] respectively. However, the films deposited using these precursors contain high carbon and oxygen impurities, and non-stoichiometric M/N ratios. The poor deposition chemistry is due to their covalent M–C bonds, which makes it difficult to remove all the methyl ligands from the deposited surface species with NH_3 at low temperatures. Alternatively, homoleptic In(III) and Ga(III) compounds with highly polarised M–N bonds have been investigated to improve the deposition chemistry of nitrides. The reported tricoordinated M–N bonded In(III) precursors require bulky ligands to inhibit polymerisation, leading to non-volatile or thermally unstable compounds.[16–20] Conversely, the dimeric tris(dimethylamido)Ga(III) ($(Ga(NMe_2)_3)_2$) is the only known tricoordinated M–N bonded compound with sufficient volatility for vapour deposition.[21] Recently, we used $(Ga(NMe_2)_3)_2$ and NH_3 plasma to deposit epitaxial GaN on SiC by ALD.[22] Although the films were near stoichiometric, they contained ~2.8% C impurities, likely due to the thermal instability of the metal amide surface species.[23]

Alternatively, monoanionic bidentate amidinate and guanidinate ligands have created homoleptic hexacoordinated M–N bonded In(III) and Ga(III) precursors with improved thermal stability in comparison to the previously mentioned tricoordinated examples. Their drawbacks, however, are decreased volatility and surface reactivity from increased molecular weight and a sterically crowded metal centre, respectively.[24–29] We initially used In(III) guanidinate ($In(guan)_3$), amidinate ($In(amd)_3$) and formamidinate ($In(form)_3$) compounds with NH_3 plasma to deposit polycrystalline InN by ALD.[25] In this study, we revealed the smaller endocyclic carbon substituent on the ligand back-

[a] R. Samii, Dr. N. J. O'Brien
Department of Physics, Chemistry and Biology,
Linköping University,
581 83 Linköping, Sweden
E-mail: nathan.o.brien@liu.se
[b] Dr. S. C. Buttera
Department of Chemistry,
Carleton University,
1125 Colonel By Drive, Ottawa, Ontario, K1S5B6, Canada
[c] Prof. V. Kessler
Department of Molecular Sciences,
Swedish University of Agricultural Sciences,
P.O. Box 7015, 75007 Uppsala, Sweden

[**] A previous version of this manuscript has been deposited on a preprint server (https://doi.org/10.26434/chemrxiv-2022-x0lcf).

Supporting information for this article is available on the WWW under https://doi.org/10.1002/ejic.202200161

Research Article
doi.org/10.1002/ejic.202200161

bone of $In(form)_3$ gave improved surface chemistry over $In(amd)_3$ and $In(guan)_3$. The homoleptic hexacoordinated gallium amidinate ($Ga(amd)_3$)[28] and guanidinate ($Ga(guan)_3$)[29] compounds have no reported volatility data and thus to date have not been used for vapour deposition.

Our initial InN studies led us to the triazenide ligand, which has a nitrogen atom in the endocyclic position of the ligand backbone. At the time, a small number of homoleptic hexacoordinated In(III) and Ga(III) triazenides were reported.[30–32] However, in those studies their suitability for vapour deposition was not investigated. In contrast, we recently revealed the In(III) and Ga(III) 1,3-diisopropyltriazenides **1a** and **2a** (Figure 1) and their subsequent use in ALD of InN, GaN, InGaN and In_2O_3.[33–36] It should be noted that **2a** was the first example of a homoleptic hexacoordinated M–N bonded compound used for vapour deposition. Interestingly, both compounds underwent gas-phase thermolysis at high temperatures inside the ALD reactor to give a smaller and more reactive metal species. Even though precursor decomposition is an undesired event in ALD, the *in-situ* thermolysis of these compounds was highly beneficial for film growth rate, purity, and crystalline quality of the deposited films. To further explore the thermal properties of In(III) and Ga(III) 1,3-dialkyltriazenides, we made changes to the exocyclic *N*-alkyl substituent of the ligand. This provided a series of symmetrical and unsymmetrical compounds with a range of different physical and chemical properties for future vapour deposition processes.

Herein, the synthesis, structure, and properties of ten new tris(1,3-dialkyltriazenido)M(III) compounds, where M = In and Ga is described. These new compounds were easily synthesised and purified by either recrystallisation or sublimation. All compounds were found to be volatile, and the majority gave single step volatilisation curves by thermogravimetric analysis (TGA). Differential scanning calorimetry (DSC) analysis showed all compounds gave two distinct exotherms, with the higher temperature event most likely precursor decomposition. The high volatility and unique thermal properties of these new triazenides make them highly advantageous for use in future vapour deposition processes of In and Ga containing materials.

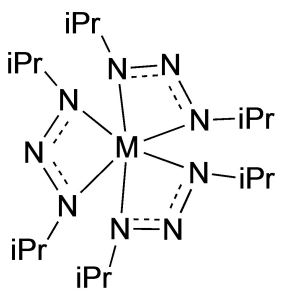

1a M = In
2a M = Ga

Figure 1. Previously reported In(III) and Ga(III) 1,3-diisopropyltriazenides **1a** and **2a**.

Results and Discussion

Synthesis and characterisation of gallium- and indium triazenide complexes

The appropriate lithiated 1,3-dialkyltriazenide ligand was prepared in the same manner as that for the aluminium triazenides.[37] Freshly prepared ligand was reacted with either $InCl_3$ or $GaCl_3$ to give compounds **1b–f** and **2b–f** (Scheme 1). All compounds except **1d** and **2d** were purified by recrystallisation to give colourless solids. Compounds **1d** and **2d** were purified by vacuum sublimation to give colourless semi-solids. Compounds **1b–f** and **2b–f** were characterised by X-ray crystallography, NMR spectroscopy, elemental analysis, sublimation temperature and, for all but semi-solids **1d** and **2d**, melting- or decomposition point. All compounds were stable when stored in solid state for months at room temperature under inert atmosphere. Exposure to air produced a white solid formed that was soluble in organic solvents. Most likely, the compounds decomposed into non-soluble mixed hydroxides and oxides.

The crystal structures of **1f** and **2f** showed hexacoordinated metal centres with three sets of chelating 1,3-di-*tert*-butyltriazenide ligands (Figure 2). The coordination geometries of the metal centres are best described as distorted octahedral. These structures are analogous to those previously reported for **1a** and **2a**.[33,34] The diffraction data showed severe disorder for ligands over a multitude of positions. Estimations from the crystal structure gave M–N bond lengths of 2.24 and 2.08 Å for **1f** and **2f**, respectively, and are comparable to **1a**, **2a** and the 1,3-diphenyltriazenide analogues.[31,33,34] Consequently, the bulky 1,3-di-*tert*-butyltriazenide ligands had no effect on the M–N distances. The optimised geometries obtained from DFT calculations agree with the crystal structures (see supporting information).

In contrast to their Al(III) analogues,[37] compounds **1b–f** and **2b–f** had sufficiently rapid exchange to yield time-averaged ^{1}H NMR spectra at room temperature (see supporting information). The faster exchange for **1a–f** and **2a–f** is explained by their longer M–N bonds, which allows for faster isomerisation *via* Rây – Dutt or Bailar twist.[38,39] Compounds with *sec*-butyl groups (**1b**, **1d**, **1e**, **2b**, **2d** and **2e**) gave two separate multiplets for the two CH_2 protons (~1.40–1.60 and 1.63–1.93 ppm). The up field multiplet (~1.40–1.60 ppm) resembled a quintet of doublets (qd) with well-defined and separated peaks for all but **2e**. This splitting pattern arises from coupling to the vicinal CH_3 and C*H* with similar coupling constants ($^3J \approx 6.6$ and 7.5 Hz, respectively). Additionally, the geminal proton splits the signal in doublets with a coupling constant, $^2J \approx 2 \cdot {}^3J$. The downfield multiplet also resembled a quintet of doublets, however, only **1b** gave a well-defined splitting pattern while **1d**, **1e**, **2b**, **2d** and **2e** showed additional splitting of each peak (< 1 Hz). This additional splitting is most likely caused by isomerism and not spin-spin coupling. This is supported by the ^{13}C NMR spectra binomial splitting patterns, where compounds with one *sec*-butyl group per ligand showed triplets (**1b**, **1e**, **2b** and **2e**), and two *sec*-butyl groups showing sextets (**1d** and **2d**).

Research Article
doi.org/10.1002/ejic.202200161

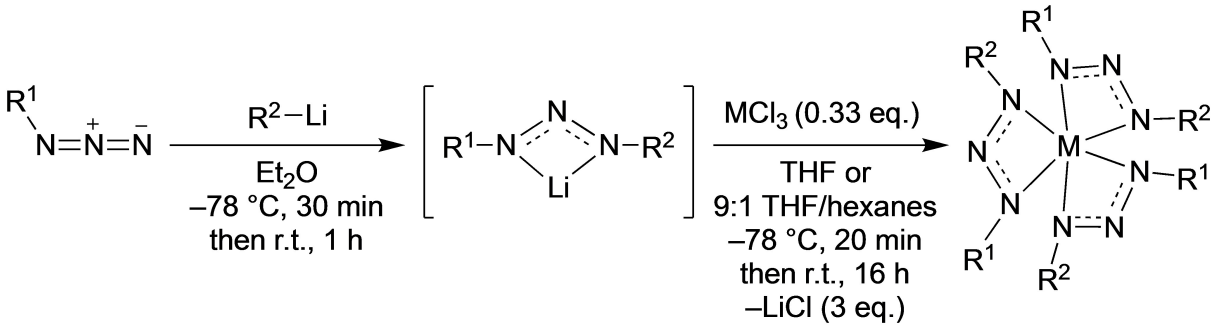

M = In	M = Ga
1a $R^1 = R^2$ = iPr (71%)	**2a** $R^1 = R^2$ = iPr (62%)
1b R^1 = iPr; R^2 = *s*Bu (60%)	**2b** R^1 = iPr; R^2 = *s*Bu (55%)
1c R^1 = iPr; R^2 = *t*Bu (69%)	**2c** R^1 = iPr; R^2 = *t*Bu (67%)
1d $R^1 = R^2$ = *s*Bu (42%)	**2d** $R^1 = R^2$ = *s*Bu (56%)
1e R^1 = *s*Bu; R^2 = *t*Bu (64%)	**2e** R^1 = *s*Bu; R^2 = *t*Bu (61%)
1f $R^1 = R^2$ = *t*Bu (80%)	**2f** $R^1 = R^2$ = *t*Bu (73%)

Scheme 1. Synthesis of In(III) and Ga(III) triazenides **1a–f** and **2a–f**.

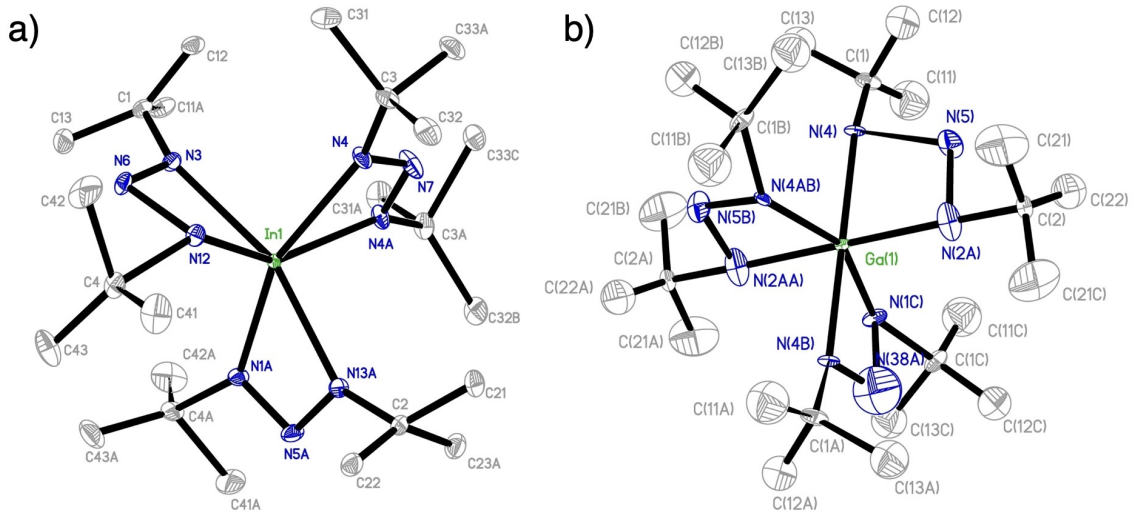

Figure 2. ORTEP drawings of the crystal structures for a) **1f** and b) **2f** with thermal ellipsoids at the 50% probability level. One of two independent molecules in the unit cell of **2f** is shown. All hydrogen atoms were omitted for clarity.

Thermal Analysis of Indium and Gallium Compounds

All compounds sublimed between 80 and 120 °C at 0.5 mbar. TGA showed single-step volatilisation with negligible residual mass for all but compound **10** (Figure 3). Triazenides **1b–f** all show improved volatility over $In(famd)_3$, which previously to **1a** was the best known hexacoordinate M–N bonded In(III) precursor for ALD.[24] Furthermore, **2b–f** along with **2a** provide the first comprehensive set of volatile hexacoordinated M–N bonded Ga(III) precursors as $Ga(amd)_3$ and $Ga(guan)_3$ have no reported volatility data.[28,29] The improved volatility of these new compounds over the literature examples can be explained by the higher electron density residing on the triazenide ligand backbone.[37,40,41] Compound **2d** showed two distinct mass-loss events and gave ~21% residual mass. Unfortunately, we were unable to obtain satisfactory elemental analysis for **2d** and thus the residual mass could be a result of impurities or precursor decomposition. The first event of **2d** volatilised at the same temperature as free *sec*-butyl-*tert*-butyltriazene,[42] while the second event occurred near that of its analogue **1d** (66–120, 180–250 °C, respectively). Compounds **2b–2e** gave comparable onsets of volatilisation to their respective In(III) analogues while

Research Article
doi.org/10.1002/ejic.202200161

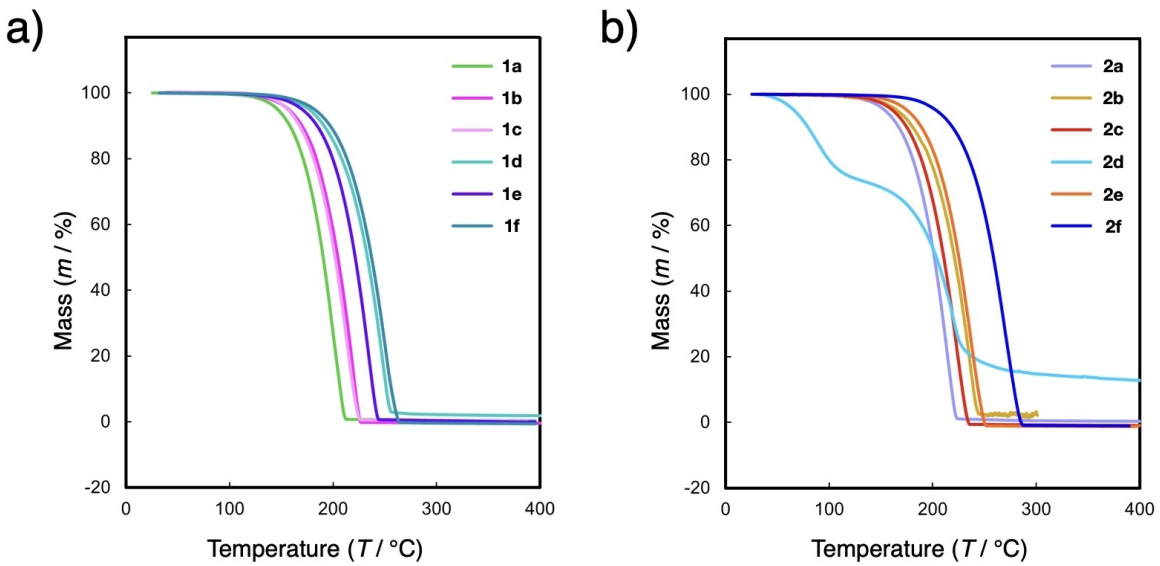

Figure 3. Thermogravimetric analysis of a) **1a–f** and b) **2a–f**.

2f differed significantly from that of **1f** (182 and 204 °C, respectively). The volatility of **1a–f** and **2a–f** was directly proportional to the number of isopropyl groups of the ligand. That is, **1a** and **2a**, with di-isopropyltriazenide ligands, were the most volatile and compounds **1d–f** and **2d–f**, without isopropyl groups, were least volatile. This correlation is attributed to the larger molecular surface area for the compounds employing the larger *tert*- and *sec*-butyl R-groups. The di-*sec*-butyltriazenides (**1d** and **2d**) gave onsets of volatility at lower temperatures than the di-*tert*-butyltriazenides (**1f** and **2f**), which is attributed to the chiral centres of the *sec*-butyl R-groups giving more disordered crystal structures. Furthermore, the asymmetrical compounds, **1e** and **2e**, gave similar onsets to **1d** and **2d**. Although structural isomers, the higher volatility of **1d**, **1e**, **2d** and **2e** over **1f** and **2f** is accredited to their lower symmetry, resulting in more disordered crystals and lower onsets of volatilisation. The compounds employing ligands with one isopropyl R-group (**1b**, **1c**, **2b** and **2c**) all gave onsets slightly above lead compounds **1a** and **2a**. The asymmetric ligand size and decreased steric bulk of these compounds, in comparison to the di-butyl derivatives (**1d–f** and **2d–2f**), gave the lowest onset of volatilisation temperatures of the new compounds. This is most likely due the unsymmetric size of the ligands, which would cause voids or irregular stacking of the compounds in solid state and would severely reduce the intermolecular dispersion forces.

DSC was employed in conjunction with melting-, and decomposition points to study the exothermic events of **1a–f** and **2a–f**. All new compounds showed two distinct exothermic events similarly to previously reported **1a** (150–180 and 220–280 °C) and **2a** (160–180 and 200–280 °C). For **1a** and **2a**, thermal studies revealed only the second exothermic event was attributed to decomposition of the precursor. Melting- and decomposition points were used to probe the new compounds, which revealed they also possessed thermal stability above the temperature range of the first DSC exothermic event. The

Table 1. Summarised thermal properties (°C) for **1a–f** and **2a–f** from vacuum sublimation (0.5 mbar), TGA and DSC.

Compound	sublimation temp.[a]	onset of volatilisation	residual mass [%]	1 Torr VP temp.	1st DSC exotherm	2nd DSC exotherm
1a	80	146	<1	134	150-180	220–280
1b	100	157	0	142	145-185	210–290
1c	100	156	0	155	170-200	245–300
1d	95	177	2	166	140-190	200–280
1e	110	170	<1	165	170-200	245–270
1f	120	182	<1	181	220-250	280–320
2a	90	154	<1	137	160-180	200–280
2b	105	166	2	152	135-170	200–280
2c	100	162	0	146	190-215	275–320
2d	85	66,[b] 180[c]	12[d]	N/A[e]	125-165	175–270
2e	100	176	0	124	175-200	225–275
2f	120	204	0	188	210-250	280–320

[a] Sublimation was performed at 0.5 mbar of pressure. [b] Refers to the onset temperature of the first volatilisation event that leads to decomposition and a second volatilisation event. [c] Refers to the onset temperature of the second volatilisation event that leads to ~21% residual mass. [d] Refers to the residual mass after the two decomposition events observed in the TGA. [e] The 1 Torr vapour pressure could not be obtained due to decomposition.

Research Article
doi.org/10.1002/ejic.202200161

temperature range of the second DSC exothermic event increased with steric bulk around the metal centre as expected. Compounds **1 f** and **2 f** gave the highest temperature range, both giving an exothermic event between 280–320 °C. Overall, all compounds in this study showed very good volatility and thermal stability for use in vapour deposition. The TGA and DSC results are summarised in Table 1.

Conclusions

In conclusion, we have synthesised a new series of In(III) and Ga(III) triazenide precursors for use in vapour deposition. The compounds were easily synthesised and purified by either crystallisation or sublimation. To our knowledge, this new family of 1,3-dialkyltriazeniedes are the most volatile hexacoordinated In(III) and Ga(III) compounds known. The high volatility and thermal stability of these In and Ga triazenides provides a series of compounds for future CVD and ALD processes.

Experimental details

Caution! As catenated nitrogen compounds are known to be associated with explosive hazards, alkylazide and compounds **1 a**–**f** and **2 a**–**f** are possible explosive energetic materials. Although we have not experienced any problems in the synthesis, characterisation, sublimation, and handling of these compounds, their energetic properties have not been fully investigated and are therefore unknown. We therefore highly recommend all appropriate standard safety precautions for handling explosive materials (safety glasses, face shield, blast shield, leather gloves, polymer apron, and ear protection) be always used when working with isopropyl-, *sec*-butyl- and *tert*-butylazide, and compounds **1 a**–**f** and **2 a**–**f**. All reactions and manipulations were carried out under a N_2 gas atmosphere on a Schlenk line using Schlenk air-free techniques or in a N_2 gas filled dry box. All anhydrous solvents were purchased from Sigma-Aldrich™ and further dried with 4 Å molecular sieves. *Tert*-butyl-, *sec*-butyl- and isopropylazide were synthesised according to the literature procedures.[43,44] $InCl_3$ (99.99 %) was purchased from Sigma-Aldrich™ and $GaCl_3$ (99.99 %) from ACROS Organics™, and both were used without further purification. Unless otherwise stated, NMR spectra were measured at room temperature with an Oxford Varian 300 or AS500 spectrometers. Solvents peaks were used as an internal standard for the ^{1}H NMR (300 MHz) and ^{13}C NMR (75 and 125 MHz) spectra. The ESI-MS data was obtained using a Thermo Scientific LCQ Fleet ESI-MS instrument. Melting points were determined in sealed capillaries on a Stuart® SMP10 melting point apparatus and are uncorrected. Elemental analysis was performed by Mikroanalytisches Laboratorium Kolbe, Germany.

General Procedure for 1,3-dialkyltriazenide In(III) and Ga(III) Complexes

Alkyllithium (3 eq.) was added to a solution of alkylazide (3 eq.) in Et_2O at −78 °C and the reaction mixture was stirred at this temperature for 30 min, then at room temperature for 1 h. This solution was then added to a solution of $InCl_3$ or $GaCl_3$ (1 eq.) in THF or 9:1 THF/*n*-hexane*, respectively, at −78 °C *via* cannula. The whole was stirred at −78 °C for 30 min, then slowly warmed to room temperature and stirred for 16 h. The reaction mixture was concentrated under reduced pressure and the resulting residue was suspended in *n*-hexane. The insoluble solids were filtered off through a pad of Celite® and the solution was concentrated under reduced pressure to give the crude product. The crude product was purified by recrystallisation from Et_2O/MeCN at −35 °C to give **1 b**–**f** and **2 b**–**f** as solids. Compound **2 d** was partially purified by vacuum sublimation. All vacuum sublimation experiments were performed at 0.5 mbar. *The solution of $GaCl_3$ in a 9:1 mixture of THF/*n*-hexane was prepared by first suspending the $GaCl_3$ in *n*-hexane and then slowly adding cold THF.

Tris(1-isopropyl-3-*sec*-butyltriazenido)indium(III) (1 b)

Compound **1 b** was synthesised according to the general procedure using *sec*-butylazide (0.72 g, 7.26 mmol) in Et_2O (40 mL), isopropyllithium (0.7 M in pentane, 10.4 mL, 7.26 mmol) and $InCl_3$ (0.54 g, 2.42 mmol) in THF (40 mL). The crude product was purified by recrystallisation to give **1 b** as a solid (0.79 g, 60 %).

1 b: Colourless solid, m.p. 177–179 °C (decomp. 235–240 °C). Sublimation: 100 °C. ^{1}H NMR (300 MHz, C_6D_6) δ 0.92 (t, J = 7.4 Hz, 9H, CH_3), 1.25 (d, J = 6.6 Hz, 18H, CH_3), 1.26 (d, J = 6.6 Hz, 9H, CH_3), 1.40–1.58 (m, 3H, CH_2), 1.63–1.80 (m, 3H, CH_2), 3.80 (sext, J = 6.7 Hz, 3H, C*H*), 4.05 (sept, J = 6.6 Hz, 3H, C*H*). ^{13}C{^{1}H} NMR (75 MHz, C_6D_6) δ 11.5 (s, CH_3), 21.3–21.7 (m, CH_3), 23.8–24.1 (m, CH_3), 31.1–31.3 (m, CH_2), 53.6 (s, C*H*), 59.8 (s, C*H*). LRMS (ESI, positive) m/z = 542 ([M + H]$^+$). Anal. calcd for $C_{21}H_{48}InN_9$: C, 46.58 %; H, 8.93 %; N, 23.28 %. Found: C, 45.58 %; H, 9.20 %; N, 23.52 %.

Tris(1-isopropyl-3-*tert*-butyltriazenido)indium(III) (1 c)

Compound **1 c** was synthesised according to the general procedure using *tert*-butylazide (0.32 g, 3.23 mmol) in Et_2O (20 mL), isopropyllithium (0.7 M in pentane, 4.61 mL, 3.23 mmol) and $InCl_3$ (0.24 g, 1.08 mmol) in THF (20 mL). The crude product was purified by recrystallisation to give **1 c** as a solid (0.40 g, 69 %).

1 c: Colourless solid, decomp. 295 °C. Sublimation: 100 °C. ^{1}H NMR (300 MHz, C_6D_6) δ 1.24 (d, J = 6.6 Hz, 18H, CH_3), 1.37 (s, 27H, CH_3), 4.04 (sept, J = 6.6 Hz, 3H, C*H*). ^{13}C{^{1}H} NMR (75 MHz, C_6D_6) δ 24.0 (s, CH_3), 30.9 (s, CH_3), 53.9 (s, C*H*), 57.1 (s, C_q). LRMS (ESI, positive) m/z = 541 ([M]$^+$). Anal. calcd for $C_{21}H_{48}InN_9$: C, 46.58 %; H, 8.93 %; N, 23.28 %. Found: C, 45.89 %; H, 9.20 %; N, 23.52 %.

Tris(1,3-di-*sec*-butyltriazenido)indium(III) (1 d)

Compound **1 d** was synthesised according to the general procedure using *sec*-butylazide (0.25 g, 2.52 mmol) in Et_2O (15 mL), *sec*-butyllithium (1.4 M in cyclohexane, 1.80 mL, 2.52 mmol) and $InCl_3$ (0.19 g, 0.84 mmol) in THF (15 mL). The crude product was purified by recrystallisation to give **1 d** as a semi-solid (0.21 g, 42 %).

1 d: Colourless semi-solid. Sublimation: 95 °C. ^{1}H NMR (300 MHz, C_6D_6) δ 0.94 (t, J = 7.5 Hz, 18H, CH_3), 1.28 (d, J = 6.0 Hz, 18H, CH_3), 1.43–1.60 (m, 6H, CH_2), 1.68–1.85 (m, 6H, CH_2), 3.79 (sext, J = 6.6 Hz, 6H, C*H*). ^{13}C{^{1}H} NMR (75 MHz, C_6D_6) δ 11.5 (s, CH_3), 21.2–21.6 (m, CH_3), 31.0–31.4 (m, CH_2), 59.7 (s, C*H*). LRMS (ESI, positive) m/z = 584 ([M + H]$^+$). Anal. calcd for $C_{24}H_{54}InN_9$: C, 49.40 %; H, 9.33 %; N, 21.60 %. Found: C, 48.67 %; H, 9.22 %; N, 21.30 %.

Tris(1-*sec*-butyl-3-*tert*-butyltriazenido)indium(III) (1 e)

Compound **1 e** was synthesised according to the general procedure using *tert*-butylazide (0.34 g, 3.43 mmol) in Et_2O (20 mL), *sec*-butyllithium (1.4 M in cyclohexane, 2.45 mL, 3.43 mmol) and $InCl_3$ (0.25 g, 1.14 mmol) in THF (20 mL). The crude product was purified by recrystallisation to give **1 e** as a solid (0.43 g, 64 %).

1e: Colourless solid, decomp. 283 °C. Sublimation: 110 °C. ^{1}H NMR (300 MHz, C_6D_6) δ 0.93 (t, J = 7.4 Hz, 9H, CH_3), 1.27 (d, J = 6.6 Hz, 9H, CH_3), 1.37 (s, 27H, CH_3), 1.41–1.59 (m, 3H, CH_2), 1.67–1.84 (m, 3H, CH_2), 3.77 (sext, J = 6.6 Hz, 3H, CH). ^{13}C{^{1}H} NMR (75 MHz, C_6D_6) δ 11.4–11.6 (m, CH_3), 21.1–21.5 (m, CH_3), 30.9 (s, CH_3) 31.1–31.4 (m, CH_2), 57.0 (s, C_q), 59.9 (s, CH). LRMS (ESI, positive) m/z = 583 ([M]$^+$). Anal. calcd for $C_{24}H_{54}InN_9$: C, 49.40 %; H, 9.33 %; N, 21.60 %. Found: C, 49.13 %; H, 9.41 %; N, 21.53 %.

Tris(1,3-di-*tert*-butyltriazenido)indium(III) (1f)

Compound **1f** was synthesised according to the general procedure using *tert*-butylazide (0.38 g, 3.83 mmol) in Et_2O (20 mL), *tert*-butyllithium (1.7 M in pentane, 2.25 mL, 3.83 mmol) and $InCl_3$ (0.28 g, 1.28 mmol) in THF (20 mL). The crude product was purified by recrystallisation to give **1f** as a solid (0.60 g, 80 %).

1f: Colourless solid, m.p. >300 °C. Sublimation: 120 °C. ^{1}H NMR (300 MHz, C_6D_6) δ 1.35 (s, 54H, CH_3). ^{13}C{^{1}H} NMR (75 MHz, C_6D_6) δ 31.0 (s, CH_3), 57.5 (s, C_q). LRMS (ESI, positive) m/z = 584 ([M + H]$^+$). Anal. calcd for $C_{24}H_{54}InN_9$: C, 49.40 %; H, 9.33 %; N, 21.60 %. Found: C, 49.20 %; H, 9.27 %; N, 21.47 %.

Tris(1-isopropyl-3-*sec*-butyltriazenido)gallium(III) (2b)

Compound **2b** was synthesised according to the general procedure using *sec*-butylazide (0.31 g, 3.13 mmol) in Et_2O (20 mL), isopropyllithium (0.7 M in pentane, 4.47 mL, 3.13 mmol) and $GaCl_3$ (0.18 g, 1.04 mmol) in THF/*n*-hexane (20 mL). The crude product was purified by recrystallisation to give **2b** as a solid (0.28 g, 55 %).

2b: Colourless solid, m.p. 178–180 °C (decomp. 255–260 °C). Sublimation: 105 °C. ^{1}H NMR (300 MHz, C_6D_6) δ 0.93 (t, J = 7.5 Hz, 9H, CH_3), 1.28 (d, J = 6.6 Hz, 18H, CH_3), 1.28 (d, J = 6.6 Hz, 9H, CH_3), 1.44–1.60 (m, 3H, CH_2), 1.73–1.90 (m, 3H, CH_2), 3.71 (sext, J = 6.7 Hz, 3H, CH), 3.95 (sept, J = 6.6 Hz, 3H, CH). ^{13}C{^{1}H} NMR (75 MHz, C_6D_6) δ 11.5 (s, CH_3), 20.6–21.9 (m, CH_3), 23.6–23.8 (m, CH_3), 30.8–31.0 (m, CH_2), 52.8 (s, CH), 59.0 (s, CH). Anal. calcd for $C_{21}H_{48}GaN_9$: C, 50.81 %; H, 9.75 %; N, 25.40 %. Found: C, 50.36 %; H, 9.71 %; N, 25.02 %.

Tris(1-isopropyl-3-*tert*-butyltriazenido)gallium(III) (2c)

Compound **2c** was synthesised according to the general procedure using *tert*-butylazide (0.39 g, 3.93 mmol) in Et_2O (20 mL), isopropyllithium (0.7 M in pentane, 5.62 mL, 3.93 mmol) and $GaCl_3$ (0.23 g, 1.31 mmol) in THF/*n*-hexane (20 mL). The crude product was purified by recrystallisation to give **2c** as a solid (0.44 g, 67 %).

2c: Colourless solid, m.p. >300 °C. Sublimation: 100 °C. ^{1}H NMR (300 MHz, C_6D_6) δ 1.27 (d, J = 6.6 Hz, 18H, CH_3), 1.37 (s, 27H, CH_3), 3.89 (sept, J = 6.6 Hz, 3H, CH). ^{13}C{^{1}H} NMR (75 MHz, C_6D_6) δ 23.7 (s, CH_3), 30.8 (s, CH_3), 52.7 (s, CH), 57.1 (s, C_q). Anal. calcd for $C_{21}H_{48}GaN_9$: C, 50.81 %; H, 9.75 %; N, 25.40 %. Found: C, 49.43 %; H, 9.79 %; N, 24.71 %.

Tris(1,3-di-*sec*-butyltriazenido)gallium(III) (2d)

Compound **2d** was synthesised according to the general procedure using *sec*-butylazide (0.31 g, 3.12 mmol) in Et_2O (20 mL), *sec*-butyllithium (1.4 M in cyclohexane, 2.23 mL, 3.12 mmol) and $GaCl_3$ (0.18 g, 1.04 mmol) in THF/*n*-hexane (20 mL). The solid was purified by sublimation at 85 °C and 0.5 mbar to give **2d** as a semi-solid (0.31 g, 56 %).

2d: Colourless semi-solid. Sublimation: 85 °C. ^{1}H NMR (300 MHz, C_6D_6) δ 0.94 (t, J = 7.5 Hz, 18H, CH_3), 1.31 (d, J = 6.7 Hz, 18H, CH_3), 1.43–1.65 (m, 6H, CH_2), 1.75–1.95 (m, 6H, CH_2), 3.70 (sext, J = 6.6 Hz, 6H, CH). ^{13}C{^{1}H} NMR (125 MHz, C_6D_6) δ 11.5 (s, CH_3), 20.6–20.9 (m, CH_3), 30.8–31.1 (m, CH_2), 58.8–58.9 (s, CH). Anal. calcd for $C_{24}H_{54}GaN_9$: C, 53.53 %; H, 10.11 %; N, 23.41 %. Found: C, 49.54 %; H, 9.32 %; N, 21.03 %.

Tris(1-*sec*-butyl-3-*tert*-butyltriazenido)gallium(III) (2e)

Compound **2e** was synthesised according to the general procedure using *tert*-butylazide (0.36 g, 3.63 mmol) in Et_2O (20 mL), *sec*-butyllithium (1.4 M in cyclohexane, 2.59 mL, 3.63 mmol) and $GaCl_3$ (0.21 g, 1.21 mmol) in THF/*n*-hexane (20 mL). The crude product was purified by recrystallisation to give **2e** as a solid (0.40 g, 61 %).

2e: Colourless solid, decomp. 280 °C. Sublimation: 100 °C. ^{1}H NMR (300 MHz, C_6D_6) δ 0.92 (t, J = 7.4 Hz, 9H, CH_3), 1.30 (d, J = 6.6 Hz, 9H, CH_3), 1.38 (s, 27H, CH_3), 1.42–1.62 (m, 3H, CH_2), 1.76–1.93 (m, 3H, CH_2), 3.64 (sext, J = 6.6 Hz, 3H, CH). ^{13}C{^{1}H} NMR (75 MHz, C_6D_6) δ 11.3–11.4 (m, CH_3), 20.4–20.5 (m, CH_3), 30.8 (s, CH_3), 30.9–30.8 (m, CH_2), 57.0 (s, C_q), 58.6 (s, CH). Anal. calcd for $C_{24}H_{54}GaN_9$: C, 53.53 %; H, 10.11 %; N, 23.41 %. Found: C, 53.38 %; H, 10.09 %; N, 23.27 %.

Tris(1,3-di-*tert*-butyltriazenido)gallium(III) (2f)

Compound **2f** was synthesised according to the general procedure using *tert*-butylazide (0.42 g, 4.24 mmol) in Et_2O (25 mL), *tert*-butyllithium (1.7 M in pentane, 2.49 mL, 4.24 mmol) and $GaCl_3$ (0.25 g, 1.41 mmol) in THF/*n*-hexane (25 mL). The crude product was purified by recrystallisation to give **2f** as a solid (0.56 g, 73 %).

2f: Colourless solid, m.p. >300 °C. Sublimation: 120 °C. ^{1}H NMR (300 MHz, C_6D_6) δ 1.39 (s, 54H, CH_3). ^{13}C{^{1}H} NMR (75 MHz, C_6D_6) δ 31.3 (s, CH_3), 58.0 (s, C_q). Anal. calcd for $C_{24}H_{54}GaN_9$: C, 53.53 %; H, 10.11 %; N, 23.41 %. Found: C, 53.01 %; H, 10.42 %; N, 23.06 %.

X-ray crystallographic data collection and structure elucidation

Single crystals of **1f** and **2f** were grown from *n*-hexane at −35 °C. The single crystals were used for X-ray diffraction data collection at 163 K on a Bruker D8 SMART Apex-II diffractometer, using graphite-monochromated Mo Kα radiation (λ = 0.71073 Å). All data were collected in a hemisphere with over 95 % completeness to $2\theta < 50.05°$. The structures were solved by direct methods. The coordinates of the metal atoms were determined from the initial solutions and the N and C atoms by subsequent differential Fourier syntheses. The solution did not contain much residual electron density, but it remained for a multitude of additional possible positions of light atoms. All non-H atoms were refined, first by isotropic and then by anisotropic approximation using Bruker SHELXTL software. The H atoms were added in a riding approximation and refined isotropically. The solutions of compounds **1f** and **2f** gave one B-level alert each, which was caused by one atom in each structure failing the Hirshfeld test. These two atoms had significantly bent thermal ellipsoids, potentially caused by more than one preferred orientation for these atoms. These ellipsoids showed no preferred orientation upon manual inspection.

TGA

TGA was performed on Pt pans with a TA instrument Q500 analyser housed in an MBraun Labmaster 130 dry box filled with N_2 gas (99.998 % purity). Pt pans were cleaned by ultrasonication, first in dilute nitric acid (~3 M), then water and 2-propanol. The pans were heated until red hot using a propane torch to remove any

remaining impurities. All TGA experiments were performed under a flow of ultrapure N_2 (99.999%, 60 sccm). For ramp experiments, samples were heated to 500 °C at a rate of 10 °C min^{-1}. The Langmuir vapour pressure equations for **1b–f** and **2b–f** were derived from the TGA data with 10 mg of mass loading using a previously reported method[45] and employing bis(2,2,6,6-tetramethyl-3,5-heptanedionato)copper(II) as the calibrant.[46] The onset of volatilisation was defined as the temperature at which 5% of the precursor mass was lost.

DSC Analysis

DSC experiments were performed using a TA Instruments DSC Q10 instrument. Inside a N_2 filled glovebox, samples of ~0.30 mg of **1b–f** and **2b–f** were sealed in Al pans. Unless otherwise stated, all samples and blank references were heated to 400 °C at a rate of 10 °C min^{-1} and N_2 (99.998%) was used as the purge gas. All experiments were performed in triplicate with similar mass loadings to ensure validity of the recorded data. Exothermic and endothermic events are indicated by positive and negative heat flow, respectively.

Quantum-chemical calculations

All quantum chemical DFT calculations were preformed using Gaussian 16 software.[47] Structural optimisation and harmonic normal mode vibrational calculations were performed using the B3LYP hybrid functional[48,49] together with Grimme's version 3 dispersion correction[50] and def2TZVP basis set.[51,52] Minimised structures were confirmed to have no imaginary frequencies.

Deposition Numbers 2157977 (for **1f**) and 2157978 (for **2f**) contain the supplementary crystallographic data for this paper. These data are provided free of charge by the joint Cambridge Crystallographic Data Centre and Fachinformationszentrum Karlsruhe Access Structures service www.ccdc.cam.ac.uk/structures.

Supporting Information

NMR spectral charts, TGA and mass loss curves, DSC data, and computational details.

Acknowledgements

The authors acknowledge Lars Ojamäe for access to the Swedish National Supercomputer Centre (NSC) and Seán Barry for use of the TGA and DSC instruments. This project was founded by the Swedish foundation for Strategic Research through the project "Time-resolved low temperature CVD for III-nitrides" (SSF-RMA 15–0018) and by the Knut and Alice Wallenberg foundation through the project "Bridging the THz gap" (No. KAW 2013.0049).

Conflict of Interest

The authors declare no conflict of interest.

Data Availability Statement

The data that support the findings of this study are available in the supplementary material of this article.

Keywords: Gallium · Indium · Precursors · Triazenides · Volatile

[1] A. G. Bhuiyan, A. Hashimoto, A. Yamamoto, *J. Appl. Phys.* **2003**, *94*, 2779–2808.
[2] K. S. A. Butcher, T. L. Tansley, *Superlattices Microstruct.* **2005**, *38*, 1–37.
[3] B. L. Liu, M. Lachab, A. Jia, A. Yoshikawaa, K. Takahashi, *J. Cryst. Growth* **2002**, *234*, 637–645.
[4] S. V. Ivanov, T. V. Shubina, T. A. Komissarova, V. N. Jmerik, *J. Cryst. Growth* **2014**, *403*, 83–89.
[5] S. M. George, *Chem. Rev.* **2010**, *110*, 111–131.
[6] N. Nepal, N. A. Mahadik, L. O. Nyakiti, S. B. Qadri, M. J. Mehl, J. K. Hite, C. R. J. Eddy, *Cryst. Growth Des.* **2013**, *13*, 1485–1490.
[7] A. Haider, S. Kizir, N. Biyikli, *AIP Adv.* **2016**, *6*, 045203.
[8] A. Wakahara, T. Tsuchiya, A. Yoshida, *J. Cryst. Growth* **1990**, *99*, 385–389.
[9] X. Feng, H. Peng, J. Gong, W. Wang, H. Liu, Z. Quan, S. Pan, L. Wang, *J. Appl. Phys.* **2018**, *124*, 243104.
[10] C. Ozgit, I. Donmez, M. Alevli, N. Biyikli, *J. Vac. Sci. Technol. A* **2012**, *30*, 01A124.
[11] P. Motamedi, N. Dalili, K. Cadien, *J. Mater. Chem. C* **2015**, *3*, 7428–7436.
[12] M. Alevli, A. Haider, S. Kizir, S. A. Leghari, N. Biyikli, *J. Vac. Sci. Technol. A* **2016**, *34*, 01A137.
[13] C. Ozgit-Akgun, E. Goldenberg, A. K. Okyay, N. Biyikil, *J. Mater. Chem. C* **2014**, *2*, 2123–2136.
[14] N. Biyikli, C. Ozgit, I. Donmez, *Nanosci. Nanotechnol. Lett.* **2012**, *4*, 1008–1014.
[15] S. Banerjee, A. A. I. Aarnink, D. J. Gravesteijn, A. Y. Kovalgin, *J. Phys. Chem. C* **2019**, *123*, 23214–23225.
[16] H. Bürger, J. Cichon, U. Goetze, U. Wannagat, H. Wismar, *J. Organomet. Chem.* **1971**, *33*, 1–12.
[17] G. Rossetto, N. Brianese, A. Camporese, M. Porchia, P. Zanella, R. Bertoncello, *Main Group Met. Chem.* **1991**, *14*, 113–122.
[18] M. A. Petrie, K. Ruhlandt-Senge, H. Hope, P. P. Power, *Bull. Soc. Chim. Fr.* **1993**, *130*, 851–855.
[19] R. Frey, V. D. Gupta, G. Linti, *Z. Anorg. Allg. Chem.* **1996**, *622*, 1060–1064.
[20] J. Kim, S. G. Bott, D. M. Hoffman, *Inorg. Chem.* **1998**, *37*, 3835–3841.
[21] K. M. Waggoner, M. M. Olmstead, P. P. Power, *Polyhedron* **1990**, *9*, 257–263.
[22] P. Rouf, N. J. O'Brien, S. C. Buttera, I. Martinovic, B. Bakhit, E. Martinsson, J. Palisaitis, C.-W. Hsu, H. Pedersen, *J. Mater. Chem. C* **2020**, *8*, 8457–8465.
[23] R. G. Gordon, in *Atomic Layer Deposition for Semiconductors* (Eds.: C. S. Hwang, C. Y. Yoo), Springer US, New York, **2014**, pp. 15–46.
[24] S. B. Kim, A. Jayaraman, D. Chua, L. M. Davis, S.-L. Zheng, X. Zhao, S. Lee, R. G. Gordon, *Chem. Eur. J.* **2018**, *24*, 9525–9529.
[25] P. Rouf, N. J. O'Brien, K. Rönnby, R. Samii, I. G. Ivanov, L. Ojamäe, H. Pedersen, *J. Phys. Chem. C* **2019**, *123*, 25691–25700.
[26] M. Gebhard, M. Hellwig, H. Parala, K. Xu, M. Winter, A. Devi, *Dalton Trans.* **2014**, *43*, 937–940.
[27] S. T. Barry, P. G. Gordon, M. J. Ward, M. J. Heikkila, W. H. Monillas, G. P. A. Yap, M. Ritala, M. Leskelä, *Dalton Trans.* **2011**, *40*, 9425–9430.
[28] A. L. Brazeau, G. DiLabio, K. A. Kreisel, W. Monillas, G. P. A. Yap, S. T. Barry, *Dalton Trans.* **2007**, 3297–3304.
[29] A. P. Kenney, G. P. A. Yap, D. S. Richeson, S. T. Barry, *Inorg. Chem.* **2005**, *44*, 2926–2933.
[30] J. T. Leman, A. R. Barron, *Polyhedron* **1989**, *8*, 1909–1912.
[31] J. T. Leman, H. A. Roman, A. R. Barron, *Organometallics* **1993**, *12*, 2986–2990.
[32] J. Sundermeyer, S. Pulz, F. Schroeder, (Umicore AG & Co. KG), *Metal Complexes Having Triazenido Ligands and Uses Thereof for Depositing Metals from the Gas Phase*, **2019**, WO 2019115646.
[33] N. J. O'Brien, P. Rouf, R. Samii, K. Rönnby, S. C. Buttera, C.-W. Hsu, I. G. Ivanov, V. Kessler, L. Ojamäe, H. Pedersen, *Chem. Mater.* **2020**, *32*, 4481–4489.
[34] P. Rouf, R. Samii, K. Rönnby, B. Bakhit, S. C. Buttera, I. Martinovic, L. Ojamäe, C.-W. Hsu, V. Kessler, J. Palisaitis, V. Kessler, H. Pedersen, N. J. O'Brien, *Chem. Mater.* **2021**, *33*, 3266–3275.

Research Article
doi.org/10.1002/ejic.202200161

[35] P. Rouf, J. Palisaitis, B. Bakhit, N. J. O'Brien, H. Pedersen, *J. Mater. Chem. C* **2021**, *9*, 13077–13080.
[36] P. Mpofu, P. Rouf, N. J. O'Brien, U. Forsberg, H. Pedersen, *Dalton Trans.* **2022**, *51*, 4712–4719.
[37] R. Samii, D. Zanders, S. C. Buttera, V. Kessler, L. Ojamäe, H. Pedersen, N. J. O'Brien, *Inorg. Chem.* **2021**, *60*, 4578–4587.
[38] C. S. Springer Jr, R. E. Sievers, *Inorg. Chem.* **1967**, *6*, 852–854.
[39] A. Rodger, B. F. Johnson, *Inorg. Chem.* **1988**, *27*, 3061–3062.
[40] R. Samii, D. Zanders, A. Fransson, G. Bačić, S. T. Barry, L. Ojamäe, V. Kessler, H. Pedersen, N. J. O'Brien, *Inorg. Chem.* **2021**, *60*, 12759–12765.
[41] R. Samii, A. Fransson, D. Zanders, A. Varga, S. T. Barry, L. Ojamäe, V. Kessler, N. J. O'Brien, *ChemRxiv*. **2022**, doi: 10.26434/chemrxiv-2022-33 s1j.
[42] K. Soussi, S. Mishra, E. Jeanneau, J.-M. Millet, S. Daniele, *Dalton Trans.* **2017**, *46*, 13055–13064.
[43] J. C. Bottaro, P. E. Penwell, R. J. Schmitt, *Synth. Commun.* **1997**, *27*, 1465–1467.
[44] M. Swetha, P. Venkata Ramana, S. G. Shirodkar, *Org. Prep. Proceed. Int.* **2011**, *43*, 348–353.
[45] G. V. Kunte, S. A. Shivashankar, A. M. Umarji, *Meas. Sci. Technol.* **2008**, *19*, 025704.
[46] C. Colominas, K. H. Lau, D. L. Hildenbrand, S. Crouch-Baker, A. Sanjurjo, *J. Chem. Eng. Data* **2001**, *46*, 446–450.
[47] M. J. Frisch, G. W. Trucks, H. B. Schlegel, G. E. Scuseria, M. A. Robb, J. R. Cheeseman, G. Scalmani, V. Barone, G. A. Petersson, H. Nakatsuji, X. Li, M. Caricato, A. V. Marenich, J. Bloino, B. G. Janesko, R. Gomperts, B. Mennucci, H. P. Hratchian, J. V. Ortiz, A. F. Izmaylov, J. L. Sonnenberg, D. Williams-Young, F. Ding, F. Lipparini, F. Egidi, J. Goings, B. Peng, A. Petrone, T. Henderson, D. Ranasinghe, V. G. Zakrzewski, J. Gao, N. Rega, G. Zheng, W. Liang, M. Hada, M. Ehara, K. Toyota, R. Fukuda, J. Hasegawa, M. Ishida, T. Nakajima, Y. Honda, O. Kitao, H. Nakai, T. Vreven, K. Throssell, J. Montgomery, J. A., J. E. Peralta, F. Ogliaro, M. J. Bearpark, J. J. Heyd, E. N. Brothers, K. N. Kudin, V. N. Staroverov, T. A. Keith, R. Kobayashi, J. Normand, K. Raghavachari, A. P. Rendell, J. C. Burant, S. S. Iyengar, J. Tomasi, M. Cossi, J. M. Millam, M. Klene, C. Adamo, R. Cammi, J. W. Ochterski, R. L. Martin, K. Morokuma, O. Farkas, J. B. Foresman, D. J. Fox, *Gaussian 16, Revision B.01*, Gaussian, Inc., Wallingford CT, **2016**.
[48] M. W. D. Hanson-Heine, M. W. George, N. A. Besley, *J. Chem. Phys.* **2013**, *138*, 064101.
[49] T. Lecklider, *EE: Eval. Eng.* **2011**, *50*, 36–39.
[50] S. Grimme, J. Antony, S. Ehrlich, H. Krieg, *J. Chem. Phys.* **2010**, *132*, 154104.
[51] F. Weigend, R. Ahlrichs, *Phys. Chem. Chem. Phys.* **2005**, *7*, 3297–3305.
[52] B. Metz, H. Stoll, M. Dolg, *J. Chem. Phys.* **2000**, *113*, 2563–2569.

Manuscript received: March 15, 2022
Revised manuscript received: July 13, 2022